Universitetet i Stavanger

DET TEKNISK-NATURVITENSKAPELIGE FAKULTET

MASTEROPPGAVE

Studieprogram/spesialisering: Konstruksjon og materialer BYGGKONSTRUKJONER	Vår semesteret, 2013 Åpen
Forfatter: Kristian Dahl	…………………………………………… (signatur forfatter)
Fagansvarlig: Jasna Bogunovic Jakobsen	
Tittel på masteroppgaven: Engelsk tittel: AEROELASTIC BEHAVIOR OF VERY LONG SPAN SUSPENSION BRIDGES	
Studiepoeng: 30	
Emneord: Suspension bridge Aeroelasicity	Sidetall: 39 + vedlegg/annet: 4 Stavanger, 17.06.13

MASTER THESIS -
KONSTRUKSJONER OG MATERIALER, BYGGKONSTRUKJONER

AEROELASTIC BEHAVIOR OF VERY LONG SPAN SUSPENSION BRIDGES
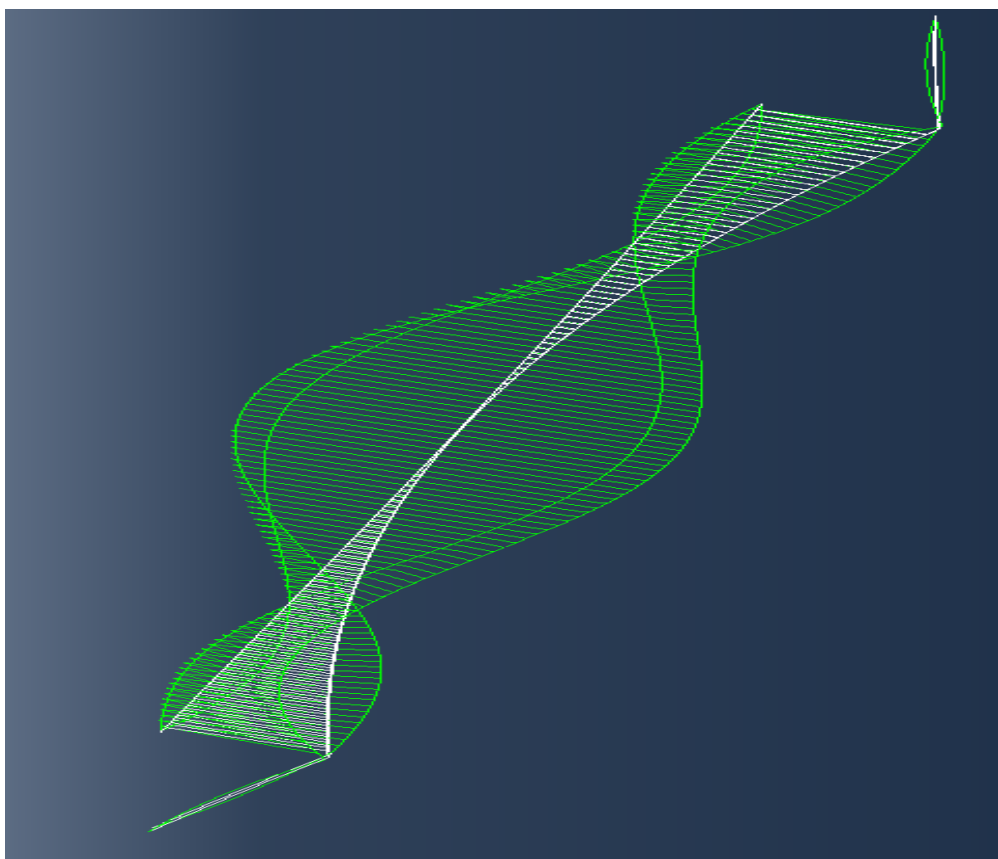
Kristian Rommetveit Dahl
215362

Summary

The main purpose of this assignment has been to obtain and understanding of the challenges concerning a future very long span suspension bridge across Sognefjorden. I have through studies of existing literature and similar bridge-projects identified the key issues for design of suspension bridges in general, and the increased challenges of span lengths beyond 3000 meter.

In short, the flutter instabilities will be the main challenge as the length of such a structure will possess very low ratios between the torsional and vertical eigenfrequencies, and the solution is to improve the aerodynamic properties of the bridge-deck.

It is also identified that the longitudinal dimension of the bridge has a stabilizing effect in regard to flutter. This should be further investigated.

Only aspects concerning the bridge-deck and main cables have been looked into.

Preface

This is the final assignment as part of a two-year master degree in Structural and Material Science at the University of Stavanger. The assignment has been carried out during the spring of 2013 and concerns the challenges in the design of the future very long span suspension bridges. This is in relation to the planned crossing of Sognefjorden where a suspension bridge with a center span of 3700 meters is one of the proposed concepts.

The main focus has been on the instability issues concerning aeroelastic effects. As this is complex theory and impossible to do without the use of wind tunnel tests, most of the assignment have been about gathering the findings of others.

Analysis has been performed in Abaqus to identify eigenmodes and –frequencies and to see the effects of varying the cross-sectional properties.

I have gained a certain understanding for the subject, and despite little sleep during these last concluding days hopefully have been able to communicate some of it.

Table of contents

1   Introduction

This assignment concerns the challenges in the design of the future very long span suspension bridges. It is in relation to a possible suspension bridge across Sognefjorden. Such a bridge requires a center span of 3700 meters and will nearly double the length of the longest suspension bridge constructed so far.

A bridge of these dimensions will be prone to various aerodynamic and structural challenges and the main object of this assignment is to obtain and understanding of these challenges.

3   Suspension Bridge – The concept

The suspension bridge is one of two main concepts for cable supported bridges, the other being the cable-stayed bridge. The main difference is where the bridge deck in the cable-stayed bridge is designed to carry the compressive force from the cables; the deck in the suspension bridge carries the transverse loading only. The main idea is however the same for both, letting the tensile strength of cables and the compressive strength of the towers carry the load of the span. As a suspended cable experiences no moment, this is by far the bridge concept that can endure the longest free spans. This makes this the ideal option for the challenges of road-design in Norway with fjord-depths of several hundred meters. The main disadvantage is the low stiffness, and relatively poor aerodynamic properties, leaving it very vulnerable to wind forces. Considerable time and effort has to be put into the aerodynamic design of suspension bridges, and wind tunnel testing is crucial for longer spans.

The main components of the suspension bridge are main cables, hangers, stiffening girder, towers and anchors.

3.1   Stiffening girder

The stiffening girder is the roadway carrying the traffic load. It consists of a series of linked boxes supported by hangers, and is constructed to sustain loads and moments between these hangers. It is the component to experience the highest wind forces, and, for short to mid-length spans, the main contributor to the torsional stiffness. For short to mid-length spans it is the main contributor to the torsional stiffness. Due to this, especially since the collapse of the Tacoma Narrows bridge, considerable effort has been, and still are, put into the studies of aerodynamic properties, leaving us the modern girders with closed streamlined-shaped boxes minimizing forces due to wind and aeroelastic effects..

Figure 3-1 The Hardangerbridge - Stiffening girder prior to installation [13]

The stiffening girder of The Sognefjord Bridge has to cover a span of 3700 m and have sail slot of 4000x70 meters.

3.2   Hangers

The hangers transfer the load from the stiffening girder to the main cables. They cannot be to close as the will experience significant wind load, but not to spread out either as they are designed for distributing the load as evenly as possible on the main cable. Another design aspect for the hangers, as well as for every component of a suspension bridge, are the eigenfrequencies, they should be different from hanger to hanger to avoid resonance of the entire system. The hangers of the Sognefjord Bridge will vary from about 370 and just under 5 meters.

3.3   Main Cables

The hangers are attached to the main cables, where the loads are transferred as transverse and axial loads. The main cables are suspended between the anchor blocks and are rests on saddles on top of the towers, and are designed for transferring the load to the ground via these. The saddles allow the cables to expand and move horizontally due to varying loads and temperatures.

The cables are assembled from multiple strands of wire into one. The steel used are constructed specifically to ensure the highest possible tensile strength and possesses twice the strength of high strength structural steels. This is ensured via the electrochemical processes and chemical composition used in the manufacturing of the cables, and they contain more than four times the carbon of ordinary structural steel. The compromise is a marginally lower modulus of elasticity and the fact that they are unfit for welding [1]

The further apart the main cables are the more they contribute to the torsional stiffness, and for very-long spans, like the proposed span across the Sognefjord, the distance between the cables play a vital role in the feasibility of the bridge.
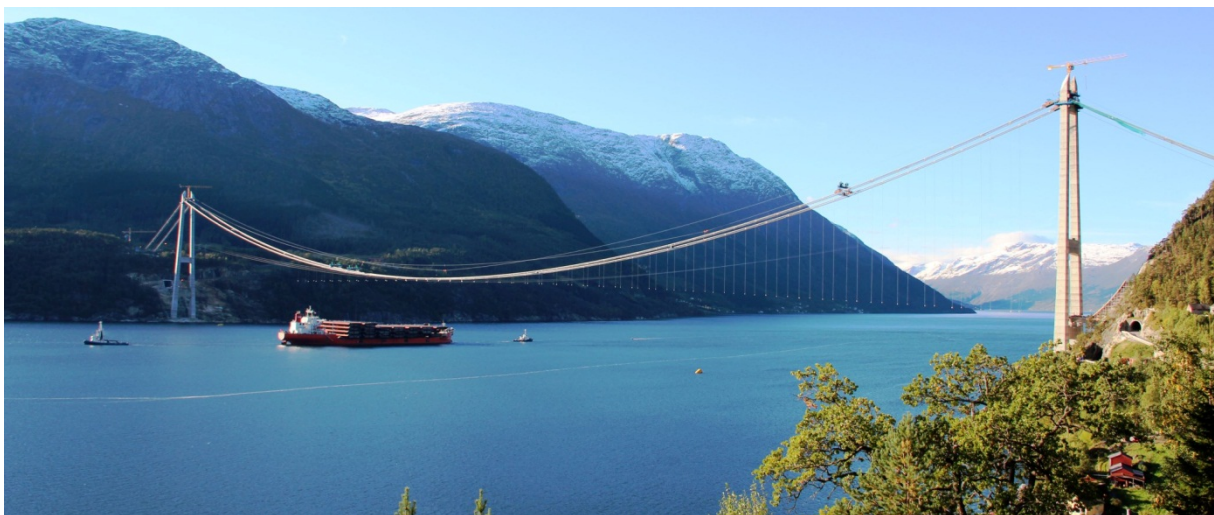

Figure 3-2 The Hardanger Bridge - Towers complete with main cables and hangers [13]

The Sognefjord Bridge will have a cable-length form anchor to anchor of a about 5747 meters.

3.4   Pylons

The main cables are laid over pylons on saddles. From here the vertical load is transferred to the ground. Due to the symmetry of the bridge the pylons experience mainly compressive axial forces and possess high capacity despite extreme slenderness. The pylons are also extremely important for the torsional stiffness to the system. For the proposed Sognefjord Bridge the pylons will consist of two 450 m high rectangular towers connected with four crossbeams. The foot of each tower will cover an area of 32x15 m^2.

3.5   Anchors

The anchors consist of a splay, and are spread even wider towards the anchoring chamber. This is where the horizontal load is supported, and due to the extreme loads the anchors are often constructed directly into mountain where possible.
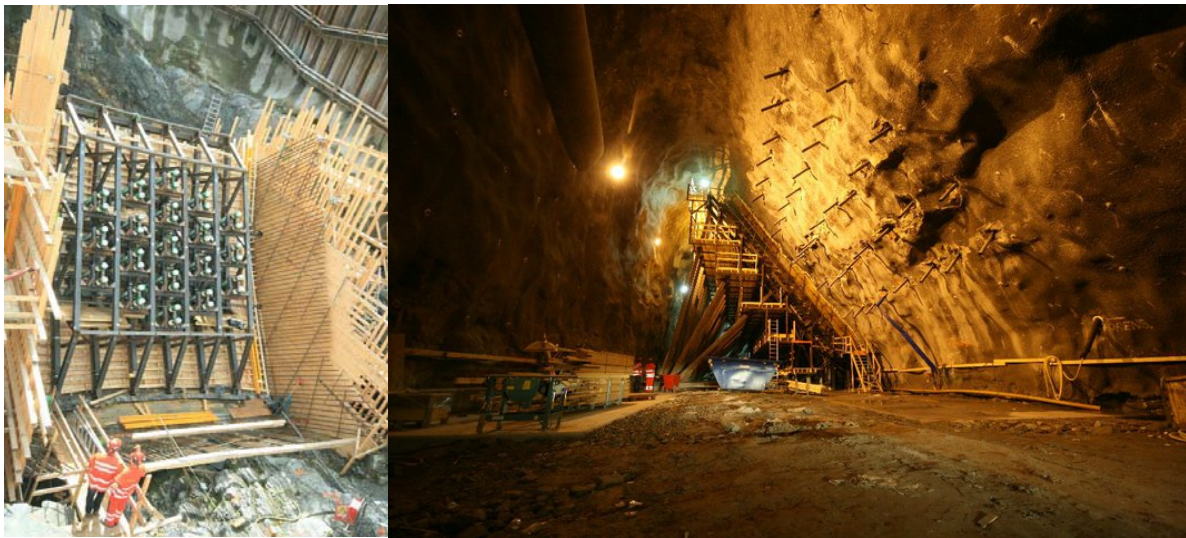
Figur 3-3 - The Hardanger bridge - Splay and anchoring chamber [13]

4 History and evolution of the suspension bridge concept

This chapter is based on information gathered in the works, of Gimsing [4], Diana [5] and Miyata [6][7].

4.1   A summary of the early years

The first modern day permanent suspension bridge in the western world, with cables made of iron was constructed in Geneva in 1823. Following, hundreds of cable similar bridges of shorter spans was erected across Europe and America during 19th century. The first major bridge, with a center span of about 500 meters, and spanning more than 1000 meters in total was the Brooklyn Bridge. It was designed by German John A. Roebling and completed in 1883. Its size and complicity seem miraculous for the time, and appears as "one of the seven wonders of the industrial age" in the BBC documentary by the same name. At a time where bridge-design was based on intuition and understanding of structural systems rather than complex mathematics, Roebling had, through his own work and investigations of prior accidents, acquired substantial knowledge of the structural

behavior of suspension bridges. The bridge is a combination of suspension bridge and a cable-stayed bridge. It is extremely over-determined and proves practically impossible to solve numerically.

After the Brooklyn Bridge, an approach based on exact mathematical theory was absorbed, leading to simpler, less redundant systems. However, all theory was based on first order effects, resulting in cumbersome structures with high depth-to-span-ratios.

The Manhattan Bridge, opened to traffic in 1909, was the first major suspension bridge based on the deflection theory. The deflection of the cable, due to the dead and traffic loads, was now accounted for. This allowed major reductions in the calculations of bending moments in the stiffening girder, thus enabling more slender stiffening girders and longer spans. Despite this break-through in the analytical approach, as it demanded complex and time-consuming calculations, no practical progress in the construction of suspension bridges was made for over 20 years.

In 1932, L.S Moisseff and F. Lienhard, introduced the effect of lateral movement into the second order theory. Now, with both the vertical and lateral deflection of the cables taken into account, practically no lateral load had to be carried by the stiffening girder. It was no longer necessary for the stiffening girder to be the stiffening element of the bridge. It was now merely the roadway, carrying the traffic load between the hangers, and had no need for any real flexural stiffness. This was yet another analytical breakthrough, but with the limited understanding of aerodynamics it should prove disastrous.

4.2 The Tacoma Narrows Bridge disaster

A well-known disaster for all engineers and engineering students is the collapse of the Tacoma Narrows Bridge.

The Tacoma Narrows Bridge (TNB) followed the Golden Gate Bridge, and was the columniation of an ever increasing trend to minimize the slenderness and depth-to-span ratios of suspension bridges. The Bridge, designed by Moisseff, was based on his own work with three-dimensional deflection theory. It had been dimensioned for traffic and static wind loads, but never for the dynamic wind loads.

As soon as the stiffening girder was erected the bridge started oscillating due to wind exposure, and was soon nicknamed "Galloping Gertie" by the construction workers [2]. For the first four months, its oscillations were purely vertical and always damped after reaching an amplitude of about 1,5 meters. As this was prior to any knowledge on fatigue, the oscillations were not considered dangerous, merely unfavorable. After four months of oscillations, the inclined cables retaining the stiffening girder in the longitudinal direction relative to the main cables broke, and the oscillations changed from vertical to torsional. The aeroelastic oscillations caused by negative aerodynamic damping twisted and turned the bridge for about an hour before the hangers snapped at the sockets, and a large part of the stiffening girder fell into the Narrows.
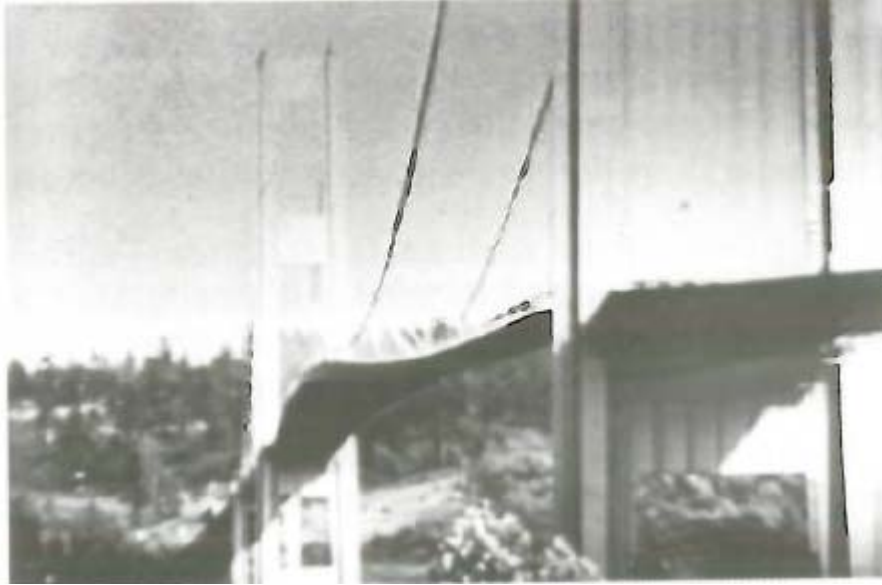
Figure 4-1 The Tacoma Narrows Bridge shortly after the onset of vibrational oscilllations [4]

The bridge had a main span of 853 meters, and an extreme depth-to-span ratio of 1:350 and width-to-span ratio of 1:72. The deck consisted of two vertical I-beams on each side of the deck, and minor transverse I-beams to carry the road-way, leaving it with practically no torsional stiffness. Combined with the poor aerodynamic properties of the design, generating large eddies, the bridge fell victim to aerodynamic instability. This created a demand for extensive studies on the subject of aerodynamic behavior, with one of the more important contributions being the studies of Freidrich Bleich and his team initiated by the United States Department of Commerce, whose work will partly be discussed later.

4.3 The streamlined-shaped box girder

The first response to this "new" aerodynamic challenge was structural. The increased understanding had designers go back to conventional bridge-design, with deep truss stiffening girders to prevent flexural and torsional vibration. It was not until 1966 that the first successful attempt to minimize the wind forces came to light, with the streamlined box girder of the Severn Bridge. The understanding of airfoil theory had led to an orthotropic wing-shaped girder. Its dimensions were similar to the TNB, with a depth of 3 meters and a depth-to-span ratio of 1:324. But the aerodynamic properties of the streamlined box, was by wind tunnel test proven superior to that of a truss girder. The closed box also proved rotationally stiffer and the Severn Bridge deck marked a revolutionary progress in bridge design.

The streamlined box girder proved both stable and cost-effective and grew foothold during the 1970s. Today it is used in most modern day medium to long span bridges.

Figur 4-2 The streamlined bridge-deck of The Great Belt Bridge during contrsuction [4]

Both the truss girder, and the closed box deck has been proved to span lengths of 1500-2000 meter with the Akashi Kaikyo and the Great Belt Bridges being the prime achievements with respective spans of 1991 and 1624 meters. However for very long spans, such as the Sognefjord Bridge, both concepts have been proven inadequate.

4.4   The "vented deck" concept

The next significant advancement in bridge design was W.C Browns "Vented Deck" concept. This deck comprised of closed boxes divided by "venting" gaps in the longitudinal direction. This allowed the wind to pass between the "beams", and thus minimizing the lift forces a regular streamlined box experiences. Its strength and aerodynamic qualities was seen as promising for the future very long span bridges.
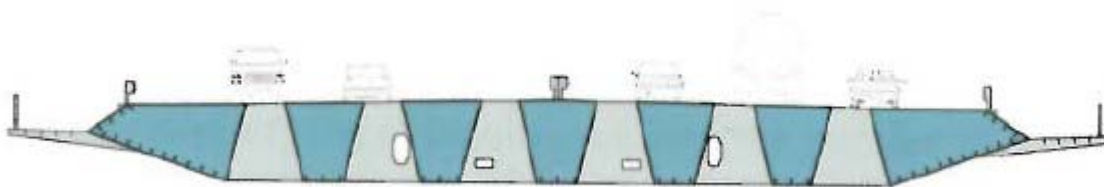
Figure 4-3 Browns "Vented Deck2 concept [4

4.5   The Akashi Kaikyo Bridge

The Akashi Kaikyo Bridge currently holds the world-record of the longest span. The multiple wind tunnel test for the bridge showed that the bridge-deck's contribution to the torsional stiffness of the system diminished as the span increased, and eventually became negligible.
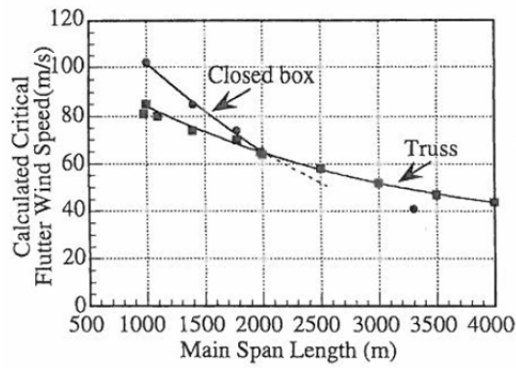
Figure 4-3 Critical flutter speed with increasing span lengths for a closed box- and a truss girder [5]

Due to limited knowledge of the time and limitations to the construction-methods they had available, they settled on a deep truss girder.
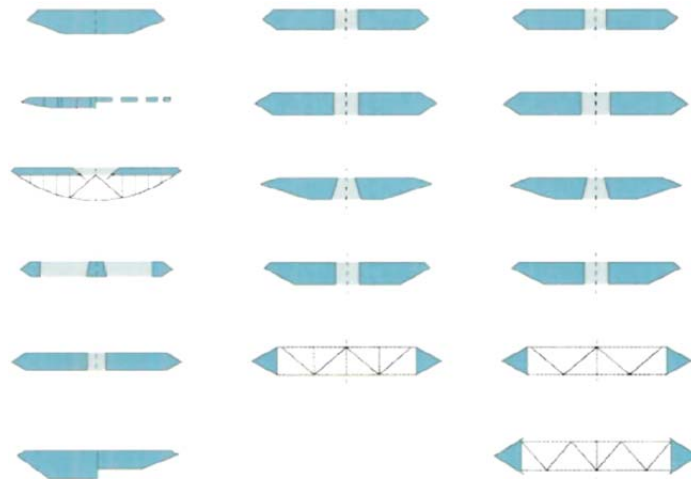
Figure 4-4 Box alternatives considered for the Akashi Bridge [4]

4.6   The Messina Strait Bridge

The Messina Strait Bridge is a complete design for a 3300 meter span bridge from Sicily to mainland Italy, but due to political and financial issues the project is currently frozen. The initial desire was to connect the island to Italy by both car and public trains.

As for the cross-section of the deck of such a span, due to previous studies of the Severn and the Akashi Kaikyo bridges, the designers knew that the key design issue would be streamlining and minimizing of the drag and lift forces. They took basis in Browns "vented deck" concept, and evolved it first to a two story deck, then to a twin deck, before due to transverse stability ended up with the tri-deck with the rail-tracks in the center of the cross-section.

9
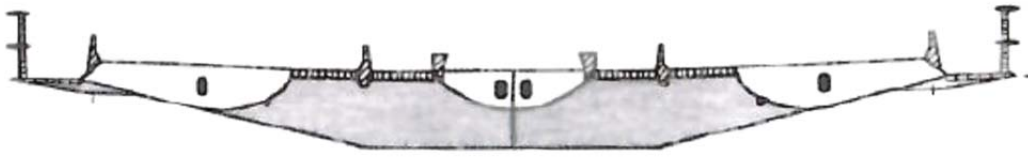
Figure 4-5 Scetch of cross-section for the Messina Bridge [4]

With soft curved bottom plates and the windward gap in a high pressure area, the air flows almost undisturbed between top and bottom ensuring minimal reaction to the wind.

4.7   The Gibraltar Bridge feasibility study

Based on previous wind tunnel tests on cross-sections meant for very long spans, a twin-box deck was chosen as the base for the low cost feasibility study for the Gibraltar Bridge. The study's most significant discovery was the link between the ratio of deck slot D and total width of solid deck B, and its effect on the critical flutter speed. They also confirmed that wind shielding by porous barriers had even better aerodynamic properties.
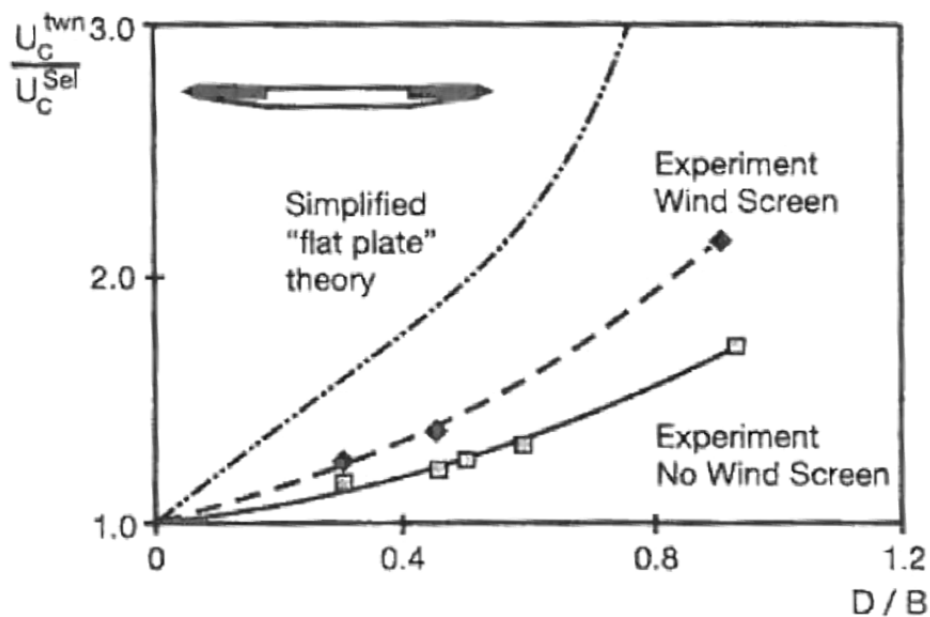
Figure 4-6 Variation of critical wind speed with deck slot / solid section width [17]

Despite finding the project feasible, the project was scrapped due to cheaper solutions using underwater tunnels.

5 Eigenfrequencies and shape modes

The TNB-disaster gave rise to comprehensive studies of structural oscillations and aerodynamics concerning suspension bridges.

One of the more influential analytical studies was performed by Friedrich Bleich and his team of engineers. As a base he used simple beam theory and, added the effect of the main cables, and developed forth degree differential equations valid for the combined system of a suspension bridge. As this proved sufficiently accurate only for asymmetric vertical oscillations, he took hold in energy methods and developed expressions for the symmetric vertical mode and both torsional modes.

5.1   The differential equation for vibration of a suspension bridge

To understand the combined system of a suspension bridge, including the action of the main cables, Blech's establishment of the fourth degree differential equation is here derived:

Looking at the stiffening girder as a simple beams subjected to a evenly distributed load we derive the differential equation for the beam alone:
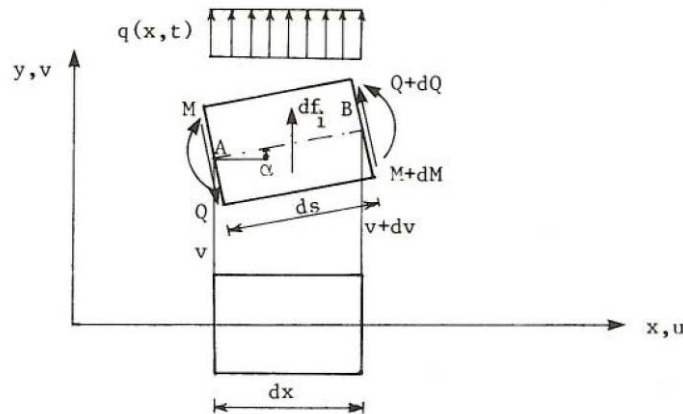
Figure-3 -1 Equilibrium of an infinite small element of a beam [15]

The deflection v is onwards substituted with η to correspond with Bleich' notations

The equilibrium of forces, including the force of inertia is then:

$$\frac{dQ}{\partial x} = -p_g(x,t) + m\ddot{\eta}$$

where $\ddot{\eta} = \frac{\partial^2 \bar{\eta}}{\partial t^2}$

(3.1)

And the equilibrium of moments:

$$Q = -\frac{\partial M}{\partial x}$$

(3.2)

11

Expressing the moment M by the curvature, $\frac{\partial^2 v}{dx^2}$, provides the differential equation:

$$EI\frac{\partial^4 \bar{\eta}_x}{dx^4} + m\frac{\partial^2 \bar{\eta}_x}{dt^2} = p_g(x,t) \qquad (3.3)$$

The evenly distributed load cause a deflection of the beam, and by elastic theory produce a "restoring force" equal to the load p_g.

Moving on to the cables, Bleich uses an expression for the horizontal cable stress to describe the vertical loads as a function of span length. The vertical loads being the mass of the system and the restoring force due to the elongation of the cables.
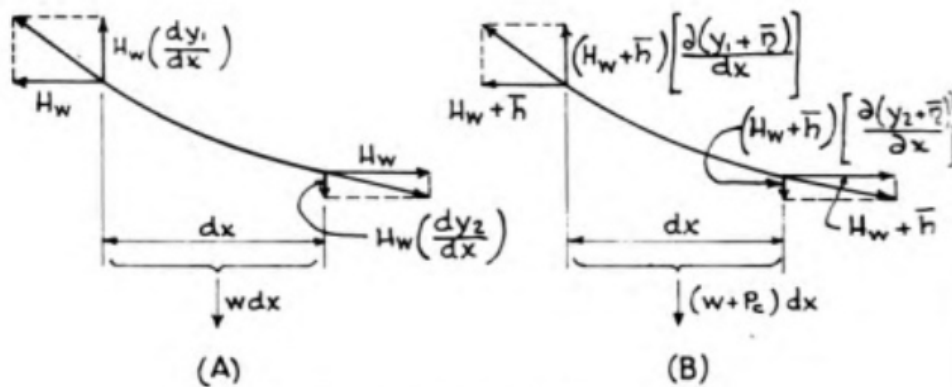
Figure 3-2 Horizontal cable stress as a function of weight an inertial loads [3]

As seen from the illustration we have

$$(w + p_c)dx = \frac{H_w + \bar{\eta}}{dx}[\partial(y_1 + \bar{\eta}_1) - \partial(y_2 + \bar{\eta}_2)] \qquad (3.4)$$

which simplifies to:

$$-p_c = H_w\frac{\partial^2 \bar{\eta}}{\partial x^2} + \bar{h}\frac{d^2 y}{dx^2} = H_w\frac{\partial^2 \bar{\eta}}{\partial x^2} - \frac{\bar{h}w}{H_w} \qquad (3.5)$$

The total inertial loads due to deflection or vibrational amplitude of the beam, is thereby:

$$p_g + p_c = E_s I\frac{d^4 \bar{\eta}_x}{dx^4} - H_w\frac{\partial^2 \bar{\eta}}{\partial x^2} + \frac{\bar{h}w}{H_w}$$
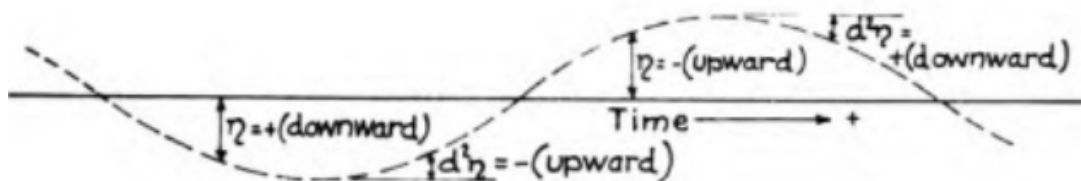
Figure 3-2 Harmonic vibration of the beam [3]

12

At the same time the acceleration of the mass opposes the deflection and for a system in equilibrium the equation of motion becomes:

$$m\frac{\partial^2 \bar{\eta}}{\partial t^2} + \left(p_g + p_c\right) = 0$$

Or (3.6)

$$\frac{w}{g}\frac{\partial^2 \bar{\eta}}{\partial t^2} + E_s I \frac{d^4 \bar{\eta}_x}{dx^4} - H_w \frac{\partial^2 \bar{\eta}}{\partial x^2} + \frac{\bar{h}w}{H_w} = 0$$

He further goes on to define the inertial forces relative to deflection of the beam as the spring constant k of the system, and introduces aerodynamically damping and external forces to the system and so on.

But the equation presented above is the basis for his analysis on the vertical asymmetric mode shapes and eigenfrequencies of a suspension bridge, and it shows how the combined mass of the system, here cables and girder, and the flexural stiffness of the beam are the governing terms.

Seeing how dependent the spring constant is to the horizontal cable force, it is easily understood that a bridge exposed to external loads, like wind-forces, will possess different eigenfrequencies than the undisturbed system.

Regarding torsional vibrations, he shed light on the poor structural properties of the slender girders of the time. As his calculations are based on a rectangular closed-box type bridge-deck, they are not applicable to the improved decks of today. But he clearly identified the combined contribution of deck and cables to the torsional stiffness and eigenfrequencies.

For the derivation of the remaining vertical and torsional mode shapes refer to his notes [3].

5.2 Very long-span suspension bridges

With increasing span-lengths follows heavier loads and increasing cable tension. From Bleich's theories it is seen that the stiffening girder's contribution to the global stiffness matrix only vary with deflection of the girder, and will at best remain constant. Meanwhile; the cables' contribution, dependent on mass, will increase with the length of the span. Eventually, the girder's contribution will become negligible, and the mode shapes and eigenfrequencies of the bridge will be equal to those of two stand-alone cables, restrained only by each other. As identified later, this is a major challenge for the design of very long-span suspension bridges.

6 Natural wind

This chapter has its base in lecture notes from the unit MKO 110 "Naturalaster" at the University of Stavanger [12] and is a short introduction to the description of natural wind and its effect on flexible structures.

6.1 Description of natural wind

Due to friction between the flow of the wind and any surface it passes over, natural wind is turbulent in both space and time. It can not be predicted and is only described statistically. It is a three-dimensional phenomenon, and seen as the mean velocity U and three, mutually orthogonal, time-dependent components, $u(t)$, $v(t)$ and $w(t)$, $u(t)$ being in the direction of U.

The design wind speed for structures is the reference wind speed for the given area, which is defined in Eurocode 1 as the wind-velocity with an annual exceedance-probability of 0,02 [7]

The stochastic processes describing turbulence is a science in itself, and way beyond the scope and complexity of this paper. However, the understanding of the wind-loads and -frequencies relevant for bridge-design demands some appreciation of the subject, and a few terms will be explained roughly.

6.2 Turbulence and Fourier series

Through Fourier series, any random repetitive signal can be decomposed into a sum of harmonic components of different frequencies. This can be visualized using the rough surface of a stormy sea. The figure below illustrates how multiple harmonic waves added together form a seemingly chaotic sea-state:
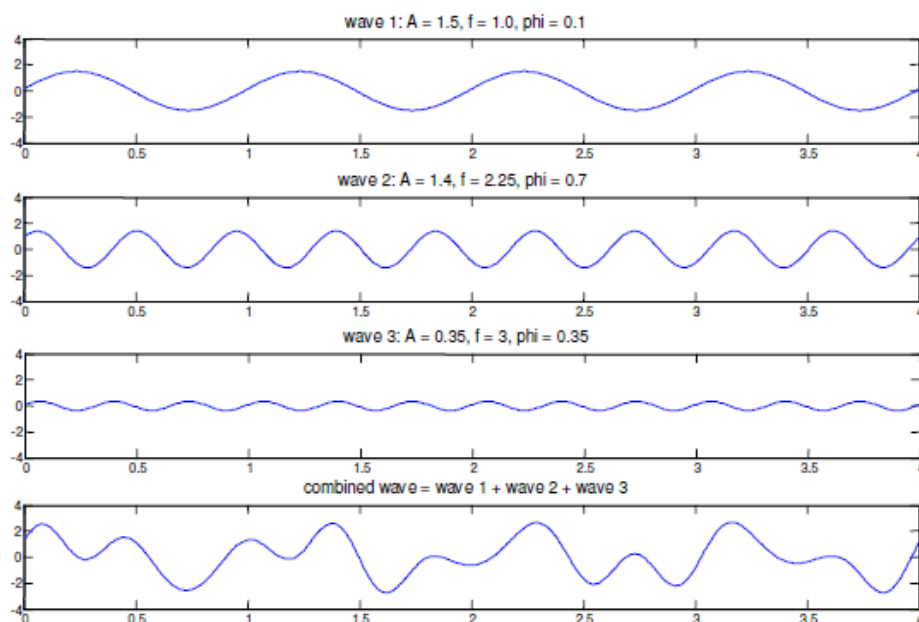
Figure 4-1 Combination of harmonic waves into a seemingly disorderly sea-state [9]

This also the case for the turbulence in wind and we can write;

$$u(t) = \sum_i A_i \cos(2\pi n_i t + \Phi_i)$$

$$v(t) = \sum_j B_j \cos(2\pi n_j t + \Phi_j) \qquad (4.1)$$

$$w(t) = \sum_k A_k \cos(2\pi n_k t + \Phi_k)$$

6.3 Turbulence intensity

The turbulence intensity is an important parameter in design of flexible structures and especially for their buffeting response which will be explained later.

It is defined as the ratio between the standard deviation of the turbulence component $\sigma_{u,v,w}$ and the mean wind speed U:

$$I_{u,v,w} = \frac{\sigma_{u,v,w}}{U} \qquad (4.2)$$

As turbulence is mainly due to the interaction between the flow and harder surfaces, its intensity decreases gradually with height.

6.4 Power-Spectral Density (PSD) function

The power spectrum, S_i, is the "distribution of turbulence with frequency" [12].

In order to retrieve and applicable representation of the power spectrum the Power-Spectral Density function proves handy.

For $u(t)$ it is defined as:

$$R_N(z,n) = \frac{n S_u(z,n)}{\sigma_u^2} \qquad (4.3)$$

For bridge-design it says in short what structural eigenfrequencies to avoid in the respective geographical area. As there are numerous applications for PSD, many forms of the function have been developed. One PSD-function fit for bridge-design is *Kaimal's Spectral Density Form*:

$$R_N(z,n) = \frac{6,8*f_L}{(1+10,2f_L)^{5/3}} \qquad (4.4)$$

where $\qquad f_L = \frac{n L_u^x(z)}{\sigma_u^2}$

and L_u^x "*a measure of the sizes of the vortices in the wind-direction, or in on the words the average size of a gust in a given direction*" [11].

This function is used in Eurocode 1, and slightly modified in Statens Vegvesen's handbook for bridge-design [10].
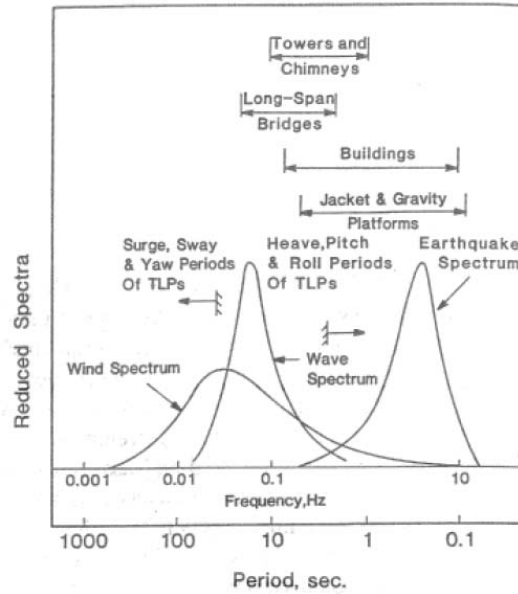
Figure 2-4 Eigenfrequencies of a long-span bridge are clearly in the frequency-area for natural wind [12]

As seen from the illustrations above, flexible structures have eigenfrequencies similar to that of turbulent wind, and it is not just severe storms and hurricanes that affect bridge-design.

There are several other important terms and functions predicting the behavior of turbulence in space and time that is important for the design of flexible structures, but they are left alone here.

7   Aerodynamic Loads

This chapter is an attempt to communicate the most relevant aspects of Prof. Hjorth-Hansens review of fluctuating forces on a line-like structure [6]. All formulas are either his or derived from his formulas.

7.1   Force coefficients

Through Bernoulli's equation we know how, a steady flow of wind onto a body creates a pressure equal to $\frac{1}{2}\rho U^2$ per unit area, where U is the velocity of the flow and ρ the density. For the two-dimensional case of a bridge deck, this pressure will create an along-wind drag-force, an orthogonal lift-force and an overturning moment about the decks longitudinal axis.
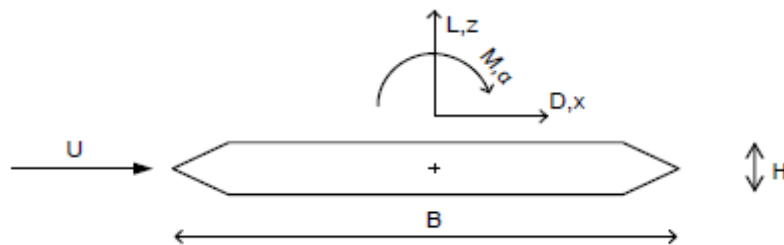
Figure 7-1 Drag, lift and overturning moment due to the mean wind-flow

$$D = \frac{1}{2}\rho U^2 D C_D$$

$$L = \frac{1}{2}\rho U^2 B C_L \qquad\qquad (7.1)$$

$$M = \frac{1}{2}\rho U^2 B^2 C_M$$

where H is exchanged with D as the height, or depth, of the bridge-deck, and $C_{D,L,M}$ are the shape coefficients of the deck in question.

The shape coefficients are dimensionless, found through wind tunnel tests and vary with the external geometry and texture of the deck. As the onset of wind produce an overturning moment M, the deck rotates, and the geometry relevant to the oncoming flow changes, hence also the shape-coefficients. In other words, the shape-coefficients are dependent on the velocity of the flow, but as seen in the graphs presented below, in a non-linear manner.
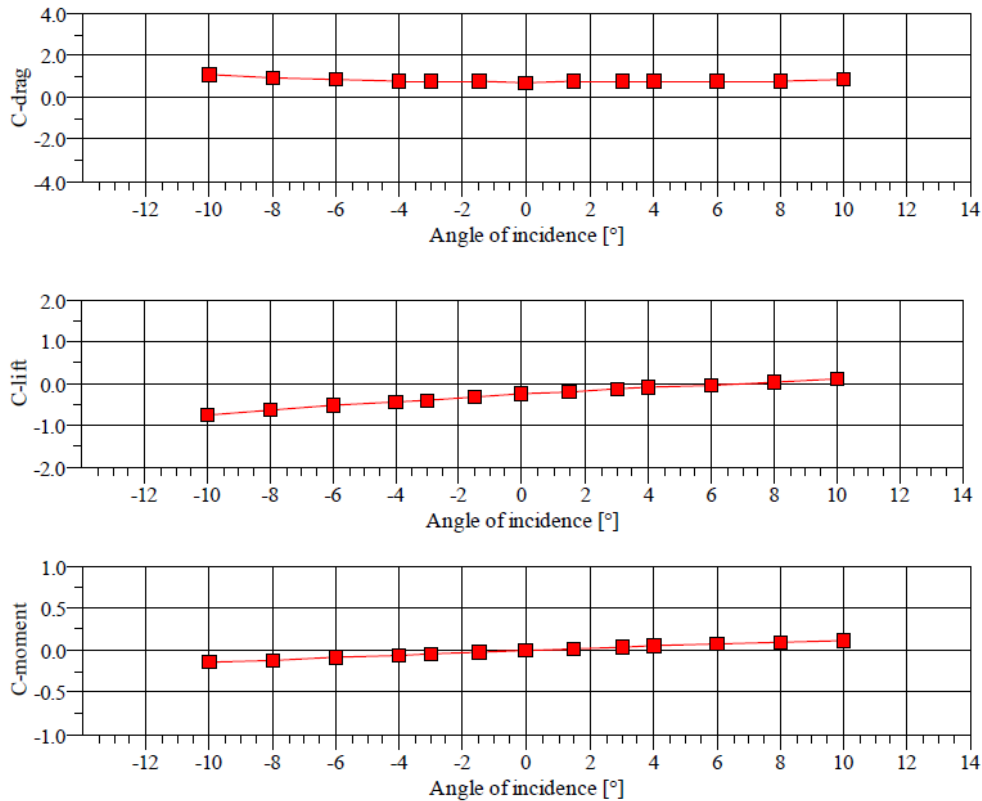
Figure 7-2 Force coefficients from the Hardanger- Bridge

α is here the "angle of attack"; the instantaneous angle of the flow relevant to the bridge-decks transverse axis.

If in possession of a powerful mathematical software, approximation by polynomials provides accurate results.

A simpler approach is to split $C_{D,L,M}(\alpha)$ into a mean and fluctuating values such that:

$$C_{D,L,M}(\alpha) = \bar{C}_{D,L,M} + \frac{\partial C_{D,L,M}}{\partial \alpha} * \alpha_f \qquad (7.2)$$

where α_f is a distance along the α-axis. This is left alone for now but are seen in the final equations.

As seen from the graph above, the slope of C_M, is positive. This means that the onset of wind will encourage a positive overturning moment of the deck, rotating it windward side up. If the mean wind is the only force of influence, the deck will eventually stabilize and we have the (short-term) mean rotational displacement of the deck, θ. This is for an ideal static load case.
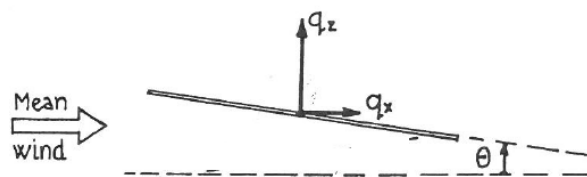
Figure 7-3 Rotation of the deck due to the mean wind [6]

18

In order to account for dynamic forces, i.e. the turbulence of the wind and the structural motion of the bridge, valid velocity- and angular arguments for the relation between the two must be established.

7.2   The angle of attack α

The relative angle between the two, α, in global coordinates simply the instantaneous angle of the vector of the wind-flow, corrected for the rotational displacement and movement of the bridge-deck.

As the base for deriving this angle of attack, we use the mean rotational displacement, θ, defined above and correct for the dynamic terms:

Fluctuating wind:
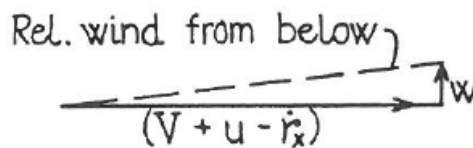
Figure 7-4 The change in α due to the vertical turbulence component w [6]

And for the horizontal and vertical motion of the deck
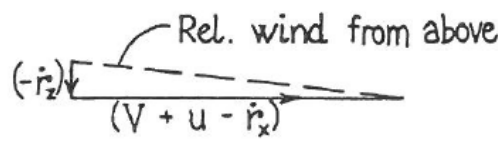
Figure 7-5   The contribution to α made by the vertical motion of the deck $\dot{r}_z$ [6]

The angle of attack will receive a contribution for the angular velocity of the the deck $\dot{\theta}$, but this is neglected here.

This provides us with the expressions for $U_{rel} = \sqrt{(U + u + \dot{r}_x)^2 + (w - \dot{r}_z)^2}$, and the angle of attack in global coordinates $\alpha = \theta + \beta = \theta + arctan \frac{w - \dot{r}_z}{U + u - \dot{r}_x}$

As U is significantly greater than all other terms involved, the angle of attack is simplified and any cross- and squared products not involving U is neglected, hence the relevant terms for aerodynamic loads are:

$$U_{rel}^2 = U^2 + 2Uu + 2U\dot{r}_x$$

and   (7.2)

$$\alpha = \theta + \frac{w - \dot{r}_z}{U}$$

The drag and lift forces are, respectively, parallel and orthogonal to the direction of U_{rel}. Therefore, again in global coordinates, the drag contributes slightly to the vertical force, and the lift slightly to the horizontal force:
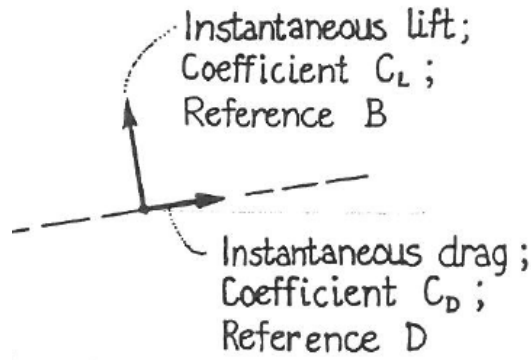
Figure 7-5 Directions of drag and lift [6]

The total sectional loads are then:

$$q_x = \frac{1}{2}\rho(U^2 + 2Uu + 2U\dot{r}_x)(C_D(\alpha)D - C_L(\alpha)B(\frac{w-\dot{r}_{z)}}{V}))$$

$$q_z = \frac{1}{2}\rho(U^2 + 2Uu + 2U\dot{r}_x)(C_L(\alpha)B + C_D(\alpha)D(\frac{w-\dot{r}_{z)}}{V}))$$ (7.3)

$$m = \frac{1}{2}\rho(U^2 + 2Uu + 2U\dot{r}_x)(C_M(\alpha)B^2)$$

7.3   Mean, fluctuation-induced and motion-induced loads

Remembering the expressions for $C_{D,L,M}(\alpha)$, it is seen that even with all the suggested simplifications, these expressions will be very complex. to make them more manageable, each expression is split into six independent expressions based on mean, motion-induced and fluctuation-induced loads as here shown by Prof. Hjorth-Hansen:

$$
\begin{array}{l|ccc}
 & q_{x,tot}\{t\} \approx & q_{z,tot}\{t\} \approx & m_{tot}\{t\} \approx \\
\hline
\text{Mean loads} & \frac{1}{2}\rho V^2\,\bar{C}_D D & \frac{1}{2}\rho V^2\,\bar{C}_L B & \frac{1}{2}\rho V^2\,\bar{C}_M B^2 \\[4pt]
\text{Fluct. loads} & -\rho V\bar{C}_D D\,\dot{r}_x & -\rho V\bar{C}_L B\,\dot{r}_x & -\rho V\bar{C}_M B^2\,\dot{r}_x \\
\text{from combina-} & & & \\
\text{tion of motion} & -\tfrac{1}{2}\rho V(C'_D D-\bar{C}_L B)\dot{r}_z & -\tfrac{1}{2}\rho V(C'_L B+\bar{C}_D D)\dot{r}_z & -\tfrac{1}{2}\rho V C'_M B^2\,\dot{r}_z \\
\text{and flow }(V\neq 0) & +\tfrac{1}{2}\rho V^2 C'_D D\,\theta_f & +\tfrac{1}{2}\rho V^2 C'_L B\,\theta_f & +\tfrac{1}{2}\rho V^2 C'_M B^2\,\theta_f \\[4pt]
\text{Fluct. from} & +\rho V\bar{C}_D D\,u & +\rho V\bar{C}_L B\,u & +\rho V\bar{C}_M B^2\,u \\
\text{wind} & & & \\
\text{turbulence} & +\tfrac{1}{2}\rho V(C'_D D-\bar{C}_L B)w & +\tfrac{1}{2}\rho V(C'_L B+\bar{C}_D D)w & +\tfrac{1}{2}\rho V C'_M B^2\,w \\[4pt]
\text{Still-air-loads} & \multicolumn{3}{c}{\text{'Added' mass and damping terms may be specified}}
\end{array}
$$

Figur 7-6 Total sectional loads on a bridge deck due to aeroelastic forces [6].

$$\tag{4.4}$$

where V is the mean load U, $\bar{C}_{D,L,M}$ is the shape coefficient due to the mean rotational angle θ, and $C'_{D,L,M} = \dfrac{\partial C_{D,L,M}}{\partial \alpha}$

This is the simplified aeroelastic load-case of a cross-sectional bridge deck.

7.4 The equation of motion

Elastic deformation of any body, generate an elastic "restoring-force" or "restoring- moment". Realizing this is the case for all displacement-dependent forces in (4.3), allows one to incorporate them into the stiffness-matrix of the bridge-deck. Similarly, all motion-dependent forces are really aerodynamic damping, and can be incorporated into the damping-matrix of the deck.

The forces due to turbulence are then the only external forces applied to the system, thus the equation of motion:

$$M_x \ddot{r}_x + [D_x + \rho \bar{C}_D D\ell V]\dot{r}_x + K_x r_x + \tfrac{1}{2}\rho C'_{D2} D\ell V\, \dot{r}_z - \tfrac{1}{2}\rho C'_D D\ell V^2 \theta \;=$$

$$M_z \ddot{r}_z + [D_z + \tfrac{1}{2}\rho C'_{L2} B\ell V]\dot{r}_z + K_z r_z + \rho \bar{C}_L B\ell V\, \dot{r}_x - \tfrac{1}{2}\rho C'_L B\ell V^2 \theta \;=$$

$$M_\theta \ddot{\theta} + D_\theta \dot{\theta} + [K_\theta - \tfrac{1}{2}\rho C'_M B^2\ell V^2]\theta + \rho \bar{C}_M B^2\ell V\, \dot{r}_x + \tfrac{1}{2}\rho C'_M B^2\ell V\, \dot{r}_z \;=$$

$$= \begin{cases} \rho \bar{C}_D D V \displaystyle\int_0^\ell u\, d\ell \;+\; \tfrac{1}{2}\rho C'_{D2} D V \displaystyle\int_0^\ell w\, d\ell \\[2ex] \rho \bar{C}_L B V \displaystyle\int_0^\ell u\, d\ell \;+\; \tfrac{1}{2}\rho C'_{L2} B V \displaystyle\int_0^\ell w\, d\ell \\[2ex] \rho \bar{C}_M B^2 V \displaystyle\int_0^\ell u\, d\ell \;+\; \tfrac{1}{2}\rho C'_M B^2 V \displaystyle\int_0^\ell w\, d\ell \end{cases}$$

Figure 7-7 The equation of motion for the bridge-deck [6]

(4.5)

Where M, D and K are the mass-, damping- and stiffness-terms respectively, l is the length of the span, $C'_{D2}D = (C'_D D - \bar{C}_L B)$ and $C'_{L2}B = (C'_L B - \bar{C}_D D)$.

Unfortunately, as the bridge will rotate and deform along the span, and the fluctuating wind forces will vary both over the cross-section and along the span, equation (4.4) and (4.5) is only an extremely simplified version of reality, fit merely as an introduction to bridge-design.

8 Aeroelastic instabilities

The identified influence of the aerodynamic forces on a system's structural damping and stiffness terms is known as aeroelasticity, and control of these interactions have proved challenging for bridge-designers over the years. Some special concerns follows.

8.1 Vortex-induced vibrations

Vortex-induced-vibrations (VIV) are encountered in relatively low-velocity smooth flow. As the flow gets separated by a slender structure, vortices are alternately shed on either side of the structure. This causes pressure variations and an alternating, harmonic force orthogonal to the wind arises.

Figure 5-1 Vortex-shedding of a sectional deck-model [4]

All bridges are somewhat exposed to VIV, but bridge-decks with sharp edges, like the old Tacoma Narrows Bridge, are particularly vulnerable.

The shedding-frequency is proportional to the ratio of the mean wind speed to the depth of the structure, and is given in Statens vegvesen's handbook for bridge-design [10] as:

$$n_s = \frac{V\,St}{h}$$

where St is Strouhal's number, found by wind tunnel tests and h is the height of the bridge deck.

If the frequency of the vortex-shedding, n_s, approaches an eigenfrequency of the structure, n_i, it can create a lock-in. The frequency of vibration now "holds on to" the shedding-frequency, and relatively large excitations of the structure may occur. After reaching a certain amplitude the vibration is always damped out, and VIV is never any immediate threat to the structure.

The critical wind speeds that may cause lock-in situations, V_r, are always to be examined and given in [10] as:

$$V_r = \frac{n_i h}{St}$$

Another parameter concerning vortex-shedding is Reynold's number. It is not relevant for most bridge decks and will not be discussed here. But as Strouhal's number depends on it, and it has great significance for the generation of vortices around the hangers and cables, it is worth mentioning. Its defined as:

$$Re = \frac{VD}{v}$$

where V is the kinematic viscosity and D the diameter of the cable [11].

8.2   Buffeting

As earlier discussed; natural wind is turbulent and inflicts fluctuating forces on to the bridge. This is called buffeting, and the behavior of the bridge due to these forces its buffeting response. As wind is always turbulent, the deck will experience buffeting. However; as turbulence by definition is chaotic, it will never "lock on" to the harmonic eigenmodes of the bridge. Any severe aeroelastic interaction will in other words never arise, and like VIV, buffeting does not comprise any immediate danger to the construction. As a fact, buffeting forces will lower the likelihood of flutter. The buffeting response is dependent on the given turbulence intensity and the structural qualities of the deck.

Although not catastrophic, VIV and buffeting can be uncomfortable for the user and are both sources to structural fatigue and hence must be damped [11].

The instabilities here mentioned below, are those that after an initial displacement continue to grow in-time and unless damped will end in catastrophic failure.

8.3   Galloping

This is a problem for bluff-type deck sections similar to that of the old Tacoma Narrows Bridge. As stated in previous chapters, the motion-dependent aerodynamic forces act as damping to the system and the total damping (here of the vertical motion is):

$$(D_z + \frac{1}{2}\rho C'_{L2} B l U)\dot{r}_z$$

where D_z is the structural damping and the remaining expression the aerodynamic damping with $C'_{L2}B = (C'_L B - \bar{C}_D D)$.

For a negatively sloping lift coefficient this expression can at a certain critical wind-speed become negative and excite movement rather than damp it. For the vertical vibration, the system now experiences the one-degree-of-freedom instability called galloping.

Although galloping might be an issue for certain elements of the bridge, i.e. the cables, it is never an issue for streamlined cross-sections as they all possess linearly increasing lift-coefficient. However; it indicates the important connection between aerodynamic instability and the derivatives of the shape factors.

Below the different force coefficients for various types of cross-sections are illustrated.
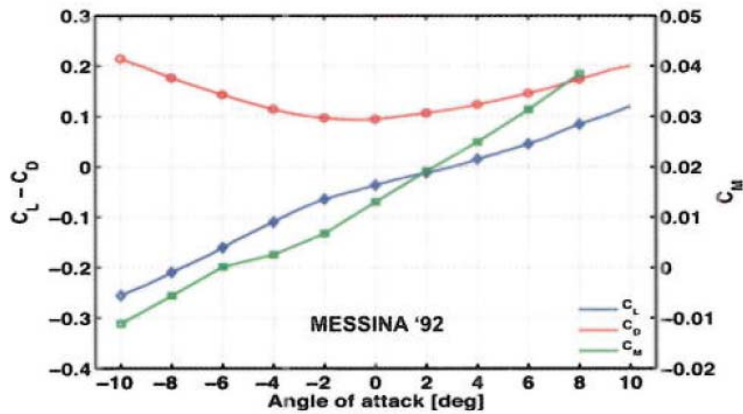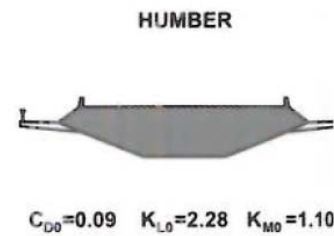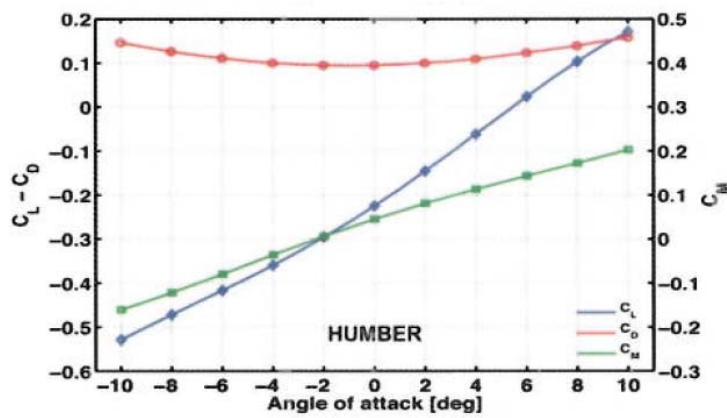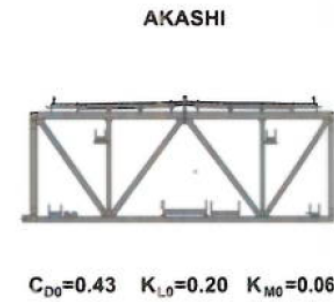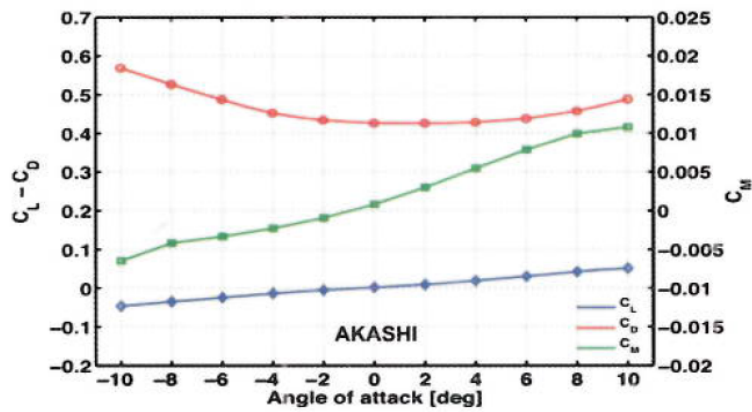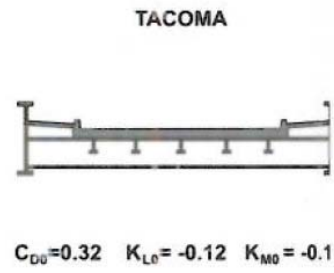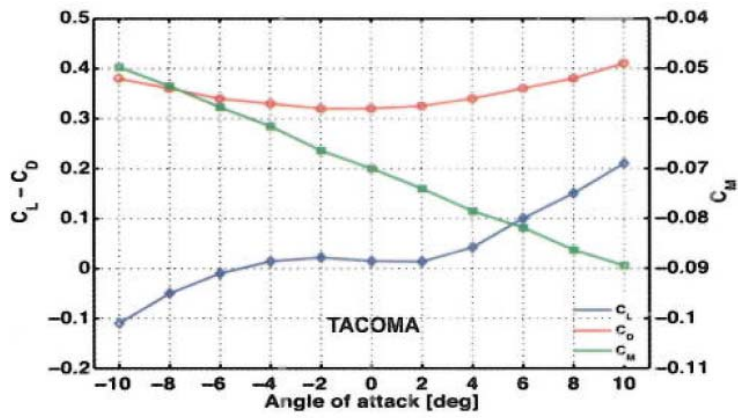
Figur 8-2 Force coefficients of various cross-sections [4]

8.4   Flutter

The two other types of instability are classic and coupled flutter, the first being pure torsional and the latter coupled vertical and torsional. As both of these involve torsional vibrations, the derivatives of the shape coefficients are constantly changing and hard to express. They are, briefly explained, given as functions of the reduced wind speed U_{red} , they differ for different cross-sections, and wind, tunnel tests are essential to determine them.

Classical flutter is associated with rectangular cross sections and the modern day streamlined bridge-decks are in general not prone to it.

Hence; the two-degree-of-freedom instability or coupled flutter is the most likely instability to be encountered for very long-span suspension bridges. It is defined by synchronized vertical and torsional vibration of the first eigenmodes of the system, and by definition the vertical and torsional frequencies have then become identical. This is possible as the aerodynamic moment caused by the onset of wind, will reduce the global torsional stiffness of the system and thereby decrease the torsional eigenfrequency $f_{1\theta}$. As f_{1v} practically remains constant, the two eigenfrequencies will approach each other, eventually become identical and produce coupled flutter [4].

The wind speed where the two frequencies connect is called the flutter speed U_f, and the ratio of $f_{1\theta}/f_{1v}$ in still air is a key factor of predicting it.

As previously identified, with increasing span-lengths the system's eigenmodes and –frequencies will approach that of two stand-alone cables, restrained only by each other. For such a system, the frequency-values are equal in still air, and torsional and vertical vibration differs only by the in-phase and out-of-phase motion of the cables. This problem has already been identified by wind tunnel tests for the proposed Messina Bridge, where a frequency-ratio of 1,36 made it very challenging to achieve an adequately high flutter speed. Comparatively the Great Belt Bridge possesses a ratio of 2,79 [4].

These instabilities are not very susceptible to structural damping, and to avoid them the aerodynamic properties of the cross-section become extremely important.

8.5   Flutter speed, U_f

To estimate the critical wind speed for flutter, the Selberg-formula [16] proves, at least for less flexible bridges, as a decent first estimate:

$$\frac{U_f}{f_\theta B} = 3,7079 \sqrt{\frac{r_g m_z}{\rho B^3}\left(1 - \left(\frac{f_v}{f_\theta}\right)^2\right)} \qquad\qquad (5.5.1)$$

where f_θ and f_v are, respectively, the frequencies of the first torsional and vertical modes, B is the width, r_g is the radius of gyration, m_z is the mass moment of inertia and ρ the density of the flow.

The formula is developed for single-deck suspension bridges with frequency ratios $\frac{f_{1\theta}}{f_{1v}} > 1,5$.

As the very-long span bridges proposed so far have multi-deck cross-sections and possesses frequency ratios lower than 1,5, the formula has to be modified.

As part of the previously mentioned Gibraltar Bridge study, Larsen and Astiz developed such a formula based on wind tunnel testing. The suggested cross-sections consisted of identical decks but the slot between the decks differed.
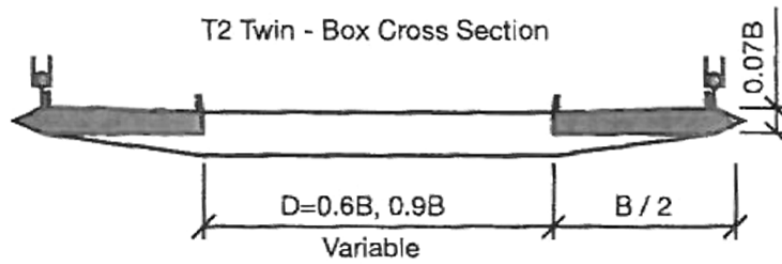
Figur 8-3 Relative twin-deck dimensions [17]

The clear link between flutter speed and the $D/B-$ratios had them modify Selberg's formula with a variable dependent on this relationship:

$$U_f^{twn} = KC_{D/B}f_\theta\sqrt{\frac{\sqrt{mI}}{\rho B}(1-(\frac{f_v}{f_\theta})^2)} \tag{5.5.2}$$

where $K = 3{,}72$, I the mass moment of inertia and $C_{D/B}$ functions of D/B adapted to the results of the U_f^{twn} found in the wind tunnel tests.

9 Wind tunnel testing

Knowing the aerodynamic properties is essential for the design of long span suspension bridges, and wind tunnel testing is the only way of establishing them accurately. Therefore a short summary is presented here [1]:

Wind tunnel test can be performed on models of entire bridges or for sectional parts of the deck.

 Cross-sectional models can be made in relatively large scale, are not too sensitive to flaws and therefore relatively cheap to manufacture. They are also easy to modify, using different guide vanes, wind barriers and so on, and proves handy for preliminary studies. Sectional models are mounted using springs to reconstruct the eigenfrequencies of the actual bridge.
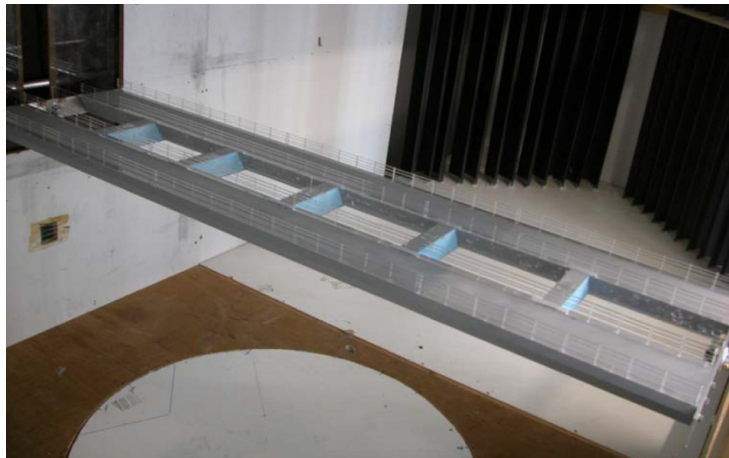
Figure 10-1 detailed sectional model [18]

Models of entire bridges on the other hand, are naturally limited to relatively small scales. This makes them tedious and expensive to manufacture as even minor flaws will affect the readings. The advantage is that they reproduce the responses of the bridge, accounting for all local and global aspects of the system.

10 Past studies on future very long span suspension bridges

Developing concepts for the future very long span suspension bridges are costly, and the way forward should be by looking backwards at lessons already learned. In this chapter some of the knowledge gained on multi-deck theory is presented.

10.1 The Gibraltar Bridge

For the low-cost feasibility study for the Gribraltar Bridge identified som keys issues for future long span bridges.

They identified coupled flutter as the main instability problem due to low frequency-ratios. As structural improvements at best have limited results, they focused their attention on improving the aerodynamic qualities of suggested twin-deck cross-section. They saw conventional methods using aerodynamic members as a solution, and as mentioned found the ratio between deck-width and deck-slot very promising. Also they confirmed using 3,5 meter high porous barriers for wind shielding improved the stability.

For a span of 3550m and a frequency-ratio of 1,43 they achieved flutter speeds of 68 m/s for the cross section and 78 m/s for the bridge.

10.2 The Messina Bridge

In the planning of the Messina Bridge they early realized that improving the aerodynamic aspects of the bridge was the way to go. They wanted to let the flow of the wind pass the bridge as undisturbed as possible, inflicting minimal load on the deck.

They used gently curved bottom-plates to reduce vortex-shedding and placed the windward side slot in a high pressure zone. This way the flow was free to from bottom- to topside, generating minimal lift and moment. Also by using a shallow deck for the mid-section hiding it behind the windward side deck, they created the effect of a twin-deck.

For a span of 3300 meters and a frequency-ratio of 1,36, they achieved flutter speeds of 70 m/s, assumedly for the cross-section.

10.3 Brusymfonien

For the case-study Brusymfonien, wind tunnel tests were performed on three twin-deck cross-sections. They consisted of same-sized decks, but had varying deck-slots of respectively 15, 20 and 30 meters. They identified that the 15 meter slot deck was prone to buffeting, while the 30 meter one was prone to VIV.

They concluded from the buffeting tests that the frequency-ratio had little influence on flutter speed, but that increasing the slot from 15-30 meters more than doubled it.

They too found guide vanes beneficial, increasing flutter values by 30-40%.

11 Analysis of the Sognefjord Bridge

For the analysis of The Sognefjord Bridge I used the softwares Abaqus/CAE and Matchad. The following analysis was conducted:

11.1   Analysis conducted

- Identification of shape and frequency of the first three eigenmodes of each of the symmetric and asymmetric vertical and torsional modes using Abaqus. The vertical modes were also found using Bleich's theories.

- Subjected the model to mean wind load and identified static response

- Altered the geometry and mass of the cross-section in search for possible changes in the structural properties of the bridge.

- Calculated flutter speed using a modified version of Selberg's formula

11.2   The finite element model

The model was made in Abacus/CAE. This is software based on the Finite Element Method, and used to solve advanced static and dynamic analysis using 2nd order theory.

The model was provided by Statens vegvesen and based on cross-sectional structural properties of a proposed cross-section for the Sognefjord Bridge. The proposed cross-section is a twin-deck with streamlined closed boxes of 12,9x2,5 meter and a 7,1 meter deck-slot.

basically constructed in the following steps:

- First the hanger-loads are calculated due to the mass and desired curvature of the deck and half the mass of the hangers themselves, this is performed separately.

- The cables are then modeled in the shape of a catenary, before being assigned mass to assume the shape of stand-alone cables.

- The loads from the hangers are assigned as vertical loads, and the cables assume their final shape.

- Next the bridge-deck is added to the model, and assigned negative vertical loads due to its own mass, and equally sized positive loads due to the tension in the hangers.

- Finally the hangers are introduced, but the hanger-loads previously assigned to cables and deck kept so that no tension is inflicted onto the hangers. This ensures that cables and bridge-deck keep their initial positions.

The next step would be to introduce towers and splays, but this is a simplified model and these elements were left out and replaced by supports at the top of the imagined tower.

12 Results of analysis

12.1 Structural eigenfrequencies

The eigenfrequencies of the Sognefjord Bridge was found using the mentioned Abaqus-model provided. For later use, the frequency-ratios was calculated too.

Abaqus

	D/B-ratio		0,2751938

VA1	0,060454	TA1	0,081629
VA2	0,114904	TA2	0,158365
VA3	0,171461	TA3	0,238060
VS1	0,075587	TS1	0,096178
VS2	0,101080	TS2	0,129064
VS3	0,145028	TS3	0,200027
	TA1/VA1	**1,350261**	
	TS1/TS1	**1,27241998**	

Bleich

VA1		0,058	0,00 %
VA2		0,115	0,00 %
VA3		0,173	0,00 %
VS1		0,072	0,00 %
VS2		0,097	0,00 %
VS3		0,149	0,00 %

12.2 Deflections due to mean wind

As identified earlier, the static drag and lift-forces and overturning moment are via the force coefficients dependent on the rotational displacement of the bridge deck. As no wind tunnel test had been performed on the proposed cross-section, coefficients from a cross-section from the case-study Brusymfonien [18] was used. This cross-section had two twin deck of width 7,5 meters and deck-slot of 20 meters, quite different from the relative dimensions of the Sognefjord Bridge.

Approximated polynomials was calculated using Mathcad and were meant to be applied to the Abaqus-model by Fortan-iterations. Introducing this to Abaqus proved very difficult, and despite the aid of experienced users it proved to tedious and I had to abandon it.

The static tests performed are therefore with the force coefficents at $\alpha = 0$. As I wanted to see the deflection due to loads on the stiffening girder, no loads were inflicted to the cables. Simulations for mean wind speeds of 10m/s and 42 m/s were performed and the results retrieved:

Mean Wind Speed	Horizontal deflection		Vertical deflection	
10 m/s	0,4097	m	0,1737	m
42 m/s	7,273	m	0,5573	m

12.3 Eigenfrequencies with altered cross-sections

The modifications of the cross-sections consisted of increasing the deck-slot to respectively 21,5 and 34,4 meters. An analysis with a slight increase in mass was performed too. The new eigenfrequencies was compared to the original ones and are presented here, the interesting or questionable findings are marked red :

1 **Mass per deck** 7500kg/m
D/B-ratio 0,2751938

VA1	0,061490	101,71 %	TA1	0,083477	102,26 %
VA2	0,114640	99,77 %	TA2	0,158530	100,10 %
VA3	0,170830	99,63 %	TA3	0,238460	100,17 %
VS1	0,075042	99,28 %	TS1	0,095752	99,56 %
VS2	0,100030	98,96 %	TS2	0,128840	99,83 %
VS3	0,144490	99,63 %	TS3	0,200180	100,08 %
	TA1/VA1	**1,357572**		100,54 %	
	TS1/TS1	**1,27597175**		100,28 %	

2 **Deck-slot** 21,5
D/B 0,83333333

VA1	0,060239	99,64 %	TA1	0,073664	90,24 %
VA2	0,114810	99,92 %	TA2	0,140730	88,86 %
VA3	0,171060	99,77 %	TA3	0,225520	94,73 %
VS1	0,079192	104,77 %	TS1	0,089049	92,59 %
VS2	0,101620	100,53 %	TS2	0,117990	91,42 %
VS3	0,154920	106,82 %	TS3	0,188620	94,30 %
	TA1/VA1	**1,222849**		90,56 %	
	TS1/TS1	**1,1244739**		88,37 %	

3 **Deck-slot** 34,4
D/B 1,33333333

VA1	0,061002	100,91 %	TA1	0,082745	101,37 %
VA2	0,114700	99,82 %	TA2	0,133760	84,46 %
VA3	0,170550	99,47 %	TA3	0,201110	84,48 %
VS1	0,075252	99,56 %	TS1	0,085764	89,17 %
VS2	0,100430	99,36 %	TS2	0,113620	88,03 %
VS3	0,144610	99,71 %	TS3	0,168940	84,46 %
	TA1/VA1	**1,356419**		100,46 %	
	TS1/TS1	**1,13969083**		89,57 %	

12.4 Flutter speeds

The flutter speeds was found using the Selberg-formula modified for the Giabraltar Bridge feasibility study:

Original model	28,396	m/s
D = 34, 4m	29,796	m/s
Gibraltar Bridge	99,8	m/s

13 Discussion of the obtained results

Here follows a discussion of the results in the order seen most fit.

13.1   Deflections and mean loads

Although the calculations of force due to constant force coefficients are wrong, the deflections sound plausible. This may be due to the marginal rotation of the deck and hence marginal change to the coefficients.

13.2   Eigenfrequencies for the original and the modified cross-sections

The results obtained from the original model had no suprises. The eigenfrequecies obtained are as expected lots lower than those of regular long span suspension bridges, and the frequency-ratios are less than 1,5. It might be interesting to see that the ratio is close to that of the Messina Bridge. Having a lighter cross-section but a longer span, this sounds reasonable. For the results using Bleich's 70 year old formulas it was interesting to see that the results obtained correspond so well with the results using powerful software.

For the modified cross-sections the results obtained are somewhat inconclusive. This is probably due to inaccuracy in the alterations in the model. When expanding the deck-slot, the mass of the modell increased due to longer cross-beams. Due to this one had to calculate new hanger-loads for the input-files. This was done separately in an input-file called bjelkemodell. As the loads increased the cable deflected, and one had to iterate. As some of this is done in Microsoft Excell and some in Abaqus, one had to move between the systems, trying to achieve equilibrium and symmetry of the system. On top of it all, Abaqus seperates the decimals using punctuation marks, while Excell uses commas. This proved extremely tedious and is most likely reason to errors.

However; early on in the thesis I thought that increasing the distance between the main cables would prove beneficial for the torsional-vibrational frequency-ratio. The results here, and the theory presented in this report proves otherwise. The general trend is that increasing cable lengths makes the bridge's torsional response more similar to that of two stand alone cables, and the lower the torsional frequencies go.

If a conclusion is to be drawn, it is what others have identified before me, that modifying the structural properties is not the key to the very long suspension bridges.

For the added mass no conclusions can be drawn from these results.

13.3   Flutter speeds

The calculated flutter speeds are clearly wrong. This is due to the use of a formula adapted to a different cross section. As the aerodynamic qualities of the girder are one of the main deciders of flutter speeds this comes as no surprise. I was recently provided with a Matlab-code for calculating flutter speed based on the aerodynamic derivatives of the brusymfonien-deck with a 20 meter deck slot. Using the correct derivatives I found the flutter speed to be 117 m/s.

14 Conclusion

The main purpose of this assignment has been to obtain and understanding of the challenges concerning a future very long span suspension bridge across Sognefjorden. I have through study of existing literature learnt the key issues for design of suspension bridges in general, and the increased challenges of span lengths above 3000 meter. Here are my thoughts on the way forward:

There are as previously stated two methods of controlling instability problems, improving the structural properties or improving the aerodynamic properties of a cross-section. I have only looked into the aspects concerning the bridge-deck and main cables, and although properties of the tower, side-spans and inclined hangers might help the situation slightly it seems like a lost cause.

The Messina Bridge, the Gibraltar Bridge and Brusymfonien all conclude that the solution is minimizing the effect of wind on the structure by improving its aerodynamic properties.

The transverse dimensions for Sognefjord Bridge may prove to be help the situation, as we don't need multiple traffic-lanes and rail-tracks. But for a bridge span of 3700 meters, it has to maintain certain dimensions to stand even the static loads.

Using new material technology will most certainly be beneficial and are being looked into already. Stronger steel will for instance cause less cable tension, and reduce the torsional contribution from the cables.

From the Gibraltar-reports it is also seen that the longitudinal dimension of the bridge has a stabilizing effect in regard to flutter. This is likely due to the effect of turbulence, disturbing the harmonic vibrations. These effects should be further investigated and the three-dimensional aspect should absolutely be introduced into wind tunnel testing for very long span suspension bridges.

Reference list

1 - Gimsing, N. J. (1997). *Cable Supported Bridges. Concept and Design.* John Wiley & Sons Ltd.

2 - University of Washington. Libraries. Special Collections Division.; Museum of History and Industry (Seattle, Wash.). (2002). *www.lib.washington.edu*. Retrieved juni 9, 2013, from www.lib.washington.edu

3 - Bleich, F. (1950). *The mathematical theroy of vibration in suspension bridges; a contribution to the work of the advisory board on the investigation of suspension bridges.* Washington: Department of Commerce, Bureau of public roads.

4 - Giorgo Diana, N. J. (2010). Challenges of a Superlong Suspension Bridge. I *The Messina Strait Bridge; A challenge and a dream.* Leiden: CRC Press.

5 - T. (1998). New idea on aero-elastic coupled flutter control for very long span bridges. I A. L. Esdahl, *Bridge Aerodynamics.* Rotterdam: A.A. Balkema.

6 - E.-H. (1993). Fluctuating Drag, Lift and Overturning moment for a line-like structure predicted (primarily) from statiic, mean loads. Trondheim, Norge: Norges Tekniske Høgskole.

7 - Standard Norge. (2009). *Eurokode 1: Laster på konstruksjoner - Del 1-4: Allmenne laster - Vindlaster.* Standard Norge.

8 - E. (2006). *Design of Buildings and Bridges for Wind; A Practical Guide for ASCE-7, Standard Users and Designers of Special Structurs.* John Wiley & Sons, Inc.

9 - J. (2006). *Design of Support Structures of Offshore Wind Turbines.* Jan van der Tempel, Offoshore Engineering and DUWIND.

10 - Statens Vegvesen, Bruseksjonen, Trafikksikkerhet-, miljø- og teknologiavdelingen. (2011). *Håndbok 185, Bruprosjektering, Eurokodeutgave.* Statens Vegvesen.

11 - C. (1997). *Wind Loads on Structures.* John Wiley & Sons.

12 - J. (207). *Wind Loading of Structures.* Taylor & Francis.

13 - H. (2012). Bilder fra Hardangerbroen.

14 - J. (u.d.). Wind load on structures - lecture notes. Universitet i Stavanger.

15 - P. (1981). *Svingning av konstruksjoner.* Tapir.

16 - J. (1995). Fluctuating Wind Load and Response of a Line-Like Engineering Structure with the Emphasis on Motion-Induced Wind Forces. Trondheim: Norges Tekniske Høgskole.

17 - A. (1998). Aeroelastic considerations for the Gibraltar Bridge feasibility study. I A. L. Esdahl, *Bridge Aerodynamics.* Balkema.

18 - S.-H. (2005). *Brusymfonien.* Statens vegvesen.

19 - D. (u.d.). *Dassault Systems*. Hentet 2013 fra www.3ds.com

APPENDIX A -

EIGENFREQUENCIES

	Svv Original	Added mass	
	6680 kg/m	7500 kg/m	%
Deck-slot	7,1	7,1	
Solid deck	25,8	25,8	
D/B	0,2751938	0,275193798	
TA1/VA1	**1,350261**	**1,357572**	100,54 %
TS1/TS1	**1,27241998**	**1,275971755**	100,28 %
VA1	0,060454	0,061490	101,71 %
VA2	0,114904	0,114640	99,77 %
VA3	0,171461	0,170830	99,63 %
VS1	0,075587	0,075042	99,28 %
VS2	0,101080	0,100030	98,96 %
VS3	0,145028	0,144490	99,63 %
TA1	0,081629	0,083477	102,26 %
TA2	0,158365	0,158530	100,10 %
TA3	0,238060	0,238460	100,17 %
TS1	0,096178	0,095752	99,56 %
TS2	0,129064	0,128840	99,83 %
TS3	0,200027	0,200180	100,08 %

INCREASED WIDTH

Deck-slot	21,5		34,4	
Solid deck	25,8		25,8	
D/B	0,83333333		1,33333333	

TA1/VA1	**1,222849**	90,56 %	**1,356419**	100,46 %
TS1/TS1	**1,1244739**	88,37 %	**1,13969083**	89,57 %
VA1	0,060239	99,64 %	0,061002	100,91 %
VA2	0,114810	99,92 %	0,114700	99,82 %
VA3	0,171060	99,77 %	0,170550	99,47 %
VS1	0,079192	104,77 %	0,075252	99,56 %
VS2	0,101620	100,53 %	0,100430	99,36 %
VS3	0,154920	106,82 %	0,144610	99,71 %
TA1	0,073664	90,24 %	0,082745	101,37 %
TA2	0,140730	88,86 %	0,133760	84,46 %
TA3	0,225520	94,73 %	0,201110	84,48 %
TS1	0,089049	92,59 %	0,085764	89,17 %
TS2	0,117990	91,42 %	0,113620	88,03 %
TS3	0,188620	94,30 %	0,168940	84,46 %

Subjected to static design wind speed

42 m/s

7,1
25,8

0,2751938

TA1/VA1		**1,352607**	100,17 %
TS1/TS1		**1,27605544**	100,29 %
	VA1	0,060363	1650,76 %
	VA2	0,114690	871,20 %
	VA3	0,171320	582,34 %
	VS1	0,075466	1388,30 %
	VS2	0,101120	994,21 %
	VS3	0,144760	737,92 %
	TA1	0,081647	1105,27 %
	TA2	0,158200	561,72 %
	TA3	0,237720	398,50 %
	TS1	0,096299	961,46 %
	TS2	0,128970	708,85 %
	TS3	0,200030	471,42 %

APPENDIX B -

BLEICH'S VERTICAL EIGENFREQUENCIES

VA1	0,058	104,23 %
VA2	0,115	99,92 %
VA3	0,173	99,11 %
VS1	0,072	104,98 %
VS2	0,097	104,21 %
VS3	0,149	97,33 %

APPENDIX C

FLUTTER SPEEDS   Uf

Original model	28,396 m/s
D = 34, 4m	29,796 m/s
Gibraltar Bridge	99,8 m/s

APPENDIX D

STATIC DEFLECTIONS

Wind speed   **10 m/s**

Using force coeficients for alfa = 0
enflicts the following evenly distributed loads onto the beams

            BJELKE1,PY,164.5
            BJELKE2,PY,109.6
            BJELKE1,PZ,143.8
            BJELKE2,PZ,-48.6

Static deflections of

	U2	U3
MAXIMUM	0,4097 m	0,1737 m

Design wind speed: **42 m/s**

Using force coeficients for alfa = 0
enflicts the following evenly distributed loads onto the beams

            BJELKE1,PY,2900
            BJELKE2,PY,1934
            BJELKE1,PZ,2537
            BJELKE2,PZ,-858

Static deflections of

	U2	U3
MAXIMUM	7,273 m	0,5573 m